Spatially Resolved Measurement of Relaxation Times in a Microfabricated Vapor Cell

Andrew Horsley
Guan-Xiang Du
and Philipp Treutlein
Departement Physik
Universität Basel, Switzerland
Email: andrew.horsley@unibas.ch

Matthieu Pellaton
Christoph Affolderbach
and Gaetano Mileti
Laboratoire Temps-Fréquence, Institut de Physique
Université de Neuchâtel, Switzerland

***Abstract*—We present a new characterisation technique for atomic vapor cells, combining time-domain measurements with absorption imaging to obtain spatially resolved information on decay times, atomic diffusion and coherent dynamics. The technique is used to characterise a microfabricated Rb vapor cell, with N_2 buffer gas, placed inside a microwave cavity. High-resolution images of the population (T_1) and coherence (T_2) lifetimes in the cell are presented. Atom-wall collisions and atomic diffusion result in a 'skin' of reduced T_1 and T_2 times around the edge of the cell. The technique also allows polarisation-resolved imaging of the microwave magnetic field inside the cell. Our technique is useful for vapor cell characterisation in atomic clocks, atomic sensors, and quantum information experiments.**

I. Introduction

The use of alkali vapor cells in atomic physics has a history extending back several decades [1], and has led to important applications in precision measurement [2] and quantum information [3]. Recent years have seen great interest in newly developed miniaturised and microfabricated vapor cells, with sizes on the order of a few millimeters or smaller. Applications include miniaturised atomic clocks [4], and magnetometers measuring both DC [5] and radio-frequency [6] fields. As new applications, one of our groups has recently demonstrated imaging of microwave magnetic fields using a vapor cell [7], and detection of microwave electric fields has been reported in Ref. [8]. Thanks to microfabrication, vapor cells have been miniaturised to a point where spatially resolved information on their properties, and on the external fields applied to them, is essential to their characterisation and performance.

In this paper, we describe a new characterisation technique, applying time-domain Ramsey, and Rabi measurements and absorption imaging [9] to a microcell. Time-domain measurements in vapor cells are currently experiencing a renaissance in interest [10]. Absorption imaging is well established in use with ultracold atoms, however its use with room-temperature atoms is a relatively unexplored area. We use these tools to characterise a microfabricated vapor cell [4] and a microwave cavity designed for compact vapor cell atomic clocks [11], obtaining spatially resolved images of decay times in the cell and images of the microwave field applied to the cell.

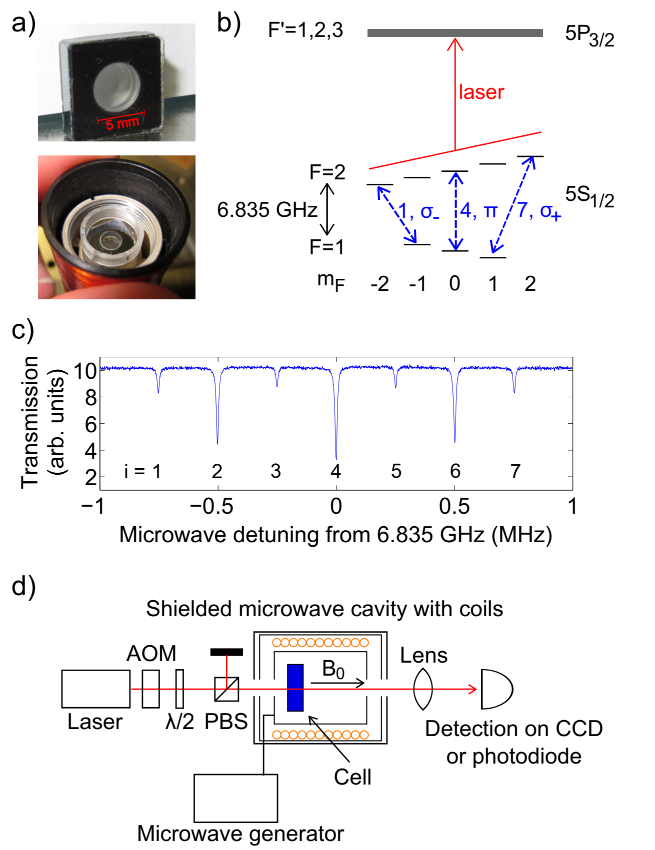

Fig. 1. a) Top: the microfabricated vapor cell used in this paper; Bottom: the cell inside the microwave cavity and coils; b) The ^{87}Rb D2 line. Due to Doppler and collisional broadening on the optical transitions, the excited state hyperfine levels F' are not resolved. Transitions between the Zeeman-split m_F levels of the ground state hyperfine structure can be individually addressed by the microwave field. The three hyperfine transitions used in this work ($i = 1, 4, 7$) are shown in dotted blue; c) A double resonance spectrum, showing laser transmission through the cell as the microwave frequency is scanned. Transmission is reduced whenever the microwave comes on resonance with a hyperfine transition; d) The experimental setup.

Readers are directed to Ref. [12] for a more in-depth coverage of this work.

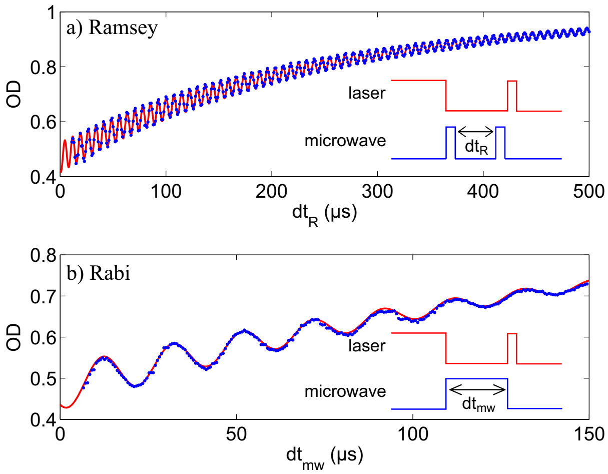

Fig. 2. Cell OD response to a) Ramsey, and b) Rabi sequences, recorded using a photodiode. Data is shown as blue dots, while the fitting curves (described in the text) are in red. Note the different scales. The insets show the laser and microwave sequences used. The OD increases with laser dark time, as the hyperfine population difference relaxes.

II. Equipment and Setup

We use the microfabricated cell shown in Figure 1a. The cell has a $5\,\mathrm{mm} \times 2\,\mathrm{mm}$ internal diameter and thickness, and contains natural abundance Rb and $63 \pm 2\,\mathrm{mbar}$ of N_2 buffer gas [4]. The cell is inserted into a microwave cavity [11], which is surrounded by a solenoid coil providing a static magnetic field (see Figure 1d). The resulting Zeeman splitting allows all seven ^{87}Rb hyperfine transitions to be individually addressed, as shown in the double-resonance spectrum of Figure 1c. We label the transitions $i = 1 \ldots 7$, in order of increasing frequency [12]. The cell temperature was set to 90°C for all data presented in this paper.

We use a laser frequency stabilised on the ^{87}Rb D2 line, pulsed using an acousto-optical modulator (AOM) to perform optical pumping [13] and absorption measurements using the single laser beam. Microwave signals near 6.835 GHz are produced by a frequency generator, and coupled into the cavity.

III. Experiment Sequences

We use pulsed Ramsey and Rabi sequences to characterize the vapor cell. Ramsey sequences provide both T_1 and T_2 times, where the T_1 times refer to population relaxation between all $F = 1$ and $F = 2$ sublevels, whilst the T_2 times are specific for the particular hyperfine m_F transition probed. Rabi sequences provide the microwave magnetic fields strengths applied to the cell.

In a typical sequence, we first apply an optical pumping pulse to the vapor that depopulates the $F = 2$ state. It is followed by microwave pulses that coherently manipulate the atomic hyperfine state. Finally, we measure the optical density (OD) in the $F = 2$ state with a probe pulse. Detection is performed using either a photodiode, or absorption imaging on a CCD camera.

We performed a first characterisation of the cell using a photodiode as the detector, described in the next two sections, III-A and III-B. An approximate laser intensity of $5\,\mathrm{mW/cm^2}$ was used.

A. Ramsey Measurements

In Ramsey sequences, we introduce two microwave pulses between the pump and probe laser pulses, separated by an evolution time dt_R (see Figure 2a). These result in coherent oscillations between the two coupled hyperfine m_F states, which we can record by scanning dt_R over multiple runs of the experiment. The oscillation frequency is given by the microwave detuning. Ramsey sequences are robust to laser and microwave field induced decoherence, as the majority of the atomic evolution occurs in the dark, with the microwave and optical fields off. As such, they provide a good measure of the T_2 time of the cell.

Figure 2a shows an example Ramsey sequence. A large-diameter laser beam was used, illuminating the entire cell, and the microwave was slightly detuned by δ from the $i = 4$ transition. The data is fit with the equation

$$\begin{aligned} \mathrm{OD} \;=\; & A - B\exp(-dt_R/T_1) \\ & + C\exp(-dt_R/T_2)\sin(\delta\, dt_R + \phi) \qquad (1) \end{aligned}$$

Where A, B, C, ϕ, T_1, T_2, and δ are fitting parameters. The fit gives the two relaxation times as $T_1 = (245 \pm 0.5)\,\mu$s and $T_2 = (322 \pm 4)\,\mu$s. The exact detuning of the microwave from resonance is given by the Ramsey oscillation frequency, $\delta = 2\pi \times (135.764 \pm 0.006)$ kHz.

B. Rabi Measurements

A Rabi sequence consists of a single microwave pulse applied during the dark time between the laser pumping and probe pulses. The microwave pulse drives Rabi oscillations between the two coupled hyperfine states, at a frequency proportional to the microwave magnetic field strength. By tuning the microwave frequency to transitions $i = 1$, 4, and 7, we are sensitive to the σ_-, π, and σ_+ components of the microwave magnetic field, respectively. This allows us to measure each vector component of the microwave magnetic field [7], [12].

An example Rabi sequence is shown in Figure 2b. A 1 mm diameter laser was used, and the microwave frequency was tuned exactly to the $i = 4$ transition, having been calibrated using a Ramsey sequence. Defining τ_1, the population difference lifetime, and τ_2, the Rabi oscillation lifetime, the data is fit with the equation

$$\begin{aligned} \mathrm{OD} \;=\; & A - B\exp(-dt_{mw}/\tau_1) \\ & + C\exp(-dt_{mw}/\tau_2)\sin(\Omega\, dt_{mw} + \phi), \qquad (2) \end{aligned}$$

where A, B, C, ϕ, τ_1, τ_2, and Ω are fitting parameters. We obtain $\tau_1 = (231 \pm 9)\,\mu$s and $\tau_2 = (94 \pm 3)\,\mu$s. On the $i = 4$ transition, we are sensitive to the π component of the microwave magnetic field, and so $\Omega_4 = 2\pi \times 50.39 \pm 0.05$ kHz corresponds to $B_\pi = 3.600 \pm 0.003\ \mu$T at the point interrogated by the laser [12].

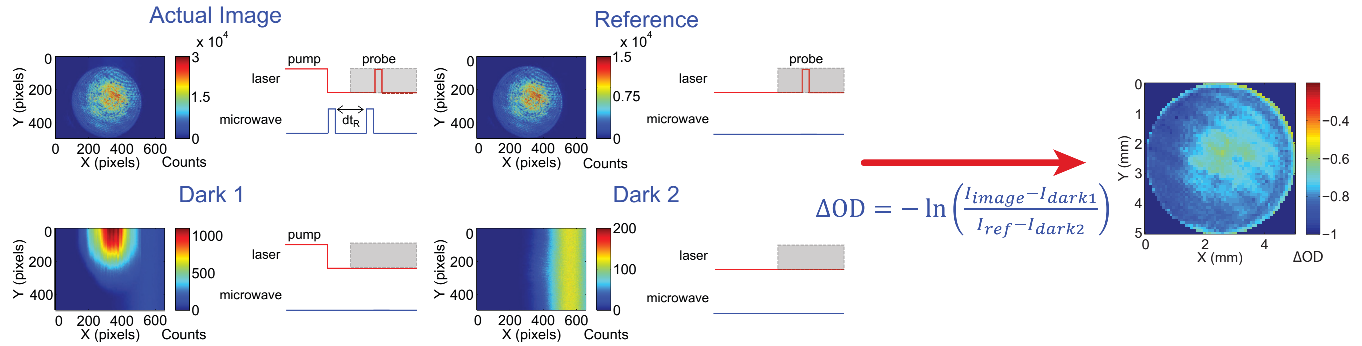

Fig. 3. Absorption imaging. Left: four images are used to create an image of the relative OD (ΔOD). These are the actual image (I_{image}), with the full experimental sequence of pumping, microwave pulses (in this example a Ramsey sequence), and probe pulse; a reference image (I_{ref}), consisting of a probe pulse, without optical pumping or microwave pulses; a dark image for the actual image (I_{dark1}), taken with pump pulse but no microwave or probe pulses; and a dark image for the reference image (I_{dark2}), taken with both the laser and microwave off. Grey boxes indicate when the camera electronic shutter is open. Right: These four images are then used to calculate ΔOD.

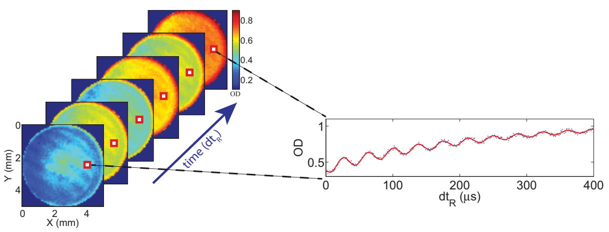

Fig. 4. Left: Images of the cell OD during a Ramsey sequence, at $dt_R = 5, 25, \ldots 105\,\mu$s. An experiment run results in an image of the optical depth for each dt timestep. Right: Examining a single pixel, we see oscillations in the OD in time, which we can fit using Eq. (1) to obtain T_1 and T_2 at that location.

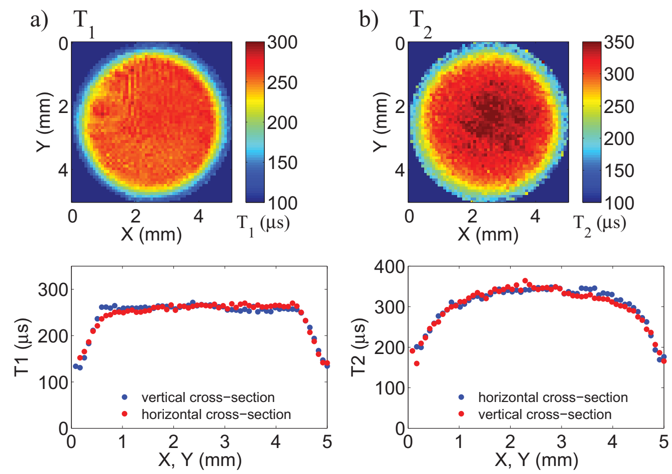

Fig. 5. Measured T_1 and T_2 times across the cell. The top panels show a) T_1 times obtained from fitting a Ramsey sequence; and b) T_2 times obtained from the same Ramsey sequence. The bottom panels show cross-sections of each image, averaged along 3 pixel wide lines passing horizontally and vertically through the image centres. Close to the walls, there is a significant decrease in T_1 and T_2 due to Rb-wall collisions.

IV. Spatially Resolved Imaging of Relaxation Times and Microwave Field Strength

We now turn our attention to measurements using the CCD camera. We use the technique of absorption imaging, which was developed in experiments with ultracold atoms to obtain accurate images of atomic density distributions in a given hyperfine state [9]. We record four images to create an image of the observed variation in optical density ΔOD, as described in Figure 3 and Ref. [12]. As a consequence of adapting the technique to hot atoms, we cannot directly obtain the OD from the four images [12], however this can in turn be obtained by normalising ΔOD to the OD measured with no optical pumping. The use of reference and dark images significantly reduces our sensitivity to short and long term drifts in the imaging system and to spatial variations in the laser intensity profile.

An image of the cell OD is produced for each dt timestep of an experimental sequence, as shown in the left-hand side of Figure 4. Each pixel has a time-varying signal (Figure 4, right-hand side), which is fit with either Eq. (1), for Ramsey sequences, or Eq. (2), for Rabi sequences.

In order to obtain a strong signal, the laser intensity averaged over the 5 mm cell diameter was set to $30\,\text{mW/cm}^2$ for the data presented in the following sections, IV-A and IV-B.

A. Imaging Relaxation

Figure 5 shows images of the T_1 and T_2 times across the cell, produced using a Ramsey sequence with the microwave frequency set slightly detuned from the $i = 4$ (clock) transition, and the microwave input power to the cavity set to 21.8 dBm,. Each pixel of the Ramsey data was fit using Eq. (1), yielding T_1 and T_2 times with $\pm 1\%$ and $\pm 4\%$ fitting uncertainties, respectively.

The bottom panels of Figure 5 show cross-sections of the T_1 and T_2 images. The relaxation rate is uniform across the centre of the cell, with T_1 times around 265 μs, and dropping away to 150 μs at the cell edge, due to the depolarisation of Rb atoms after collisions with the cell walls [12]. This 'skin' of reduced atomic lifetimes near the cell edge is reproduced in a model of the T_1 time presented in Ref. [12]. The T_1

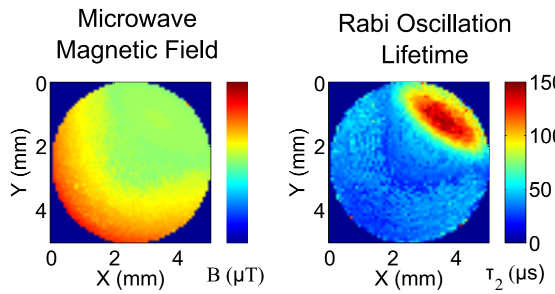

Fig. 6. Left: Image of the π component of the microwave magnetic field, obtained using a Rabi sequence on the clock transition. Right: Images of the corresponding Rabi oscillation lifetime, τ_2.

times obtained in the centre of the cell are larger than the values obtained using the photodiode in section III-A, as the photodiode measurements averaged the relaxation time over the entire cell, including the regions near the cell walls.

The T_2 time across the cell, shown in the right-hand panels of Figure 5, has a much smoother profile than the flat-top profile of the T_1 images, with the influence of the cell walls extending to the cell centre. T_2 values in the centre of the cell peak at around $350\,\mu$s.

B. Imaging the Microwave Magnetic Field

Figure 6 shows the π component of the microwave magnetic field, obtained using a Rabi measurement on the clock transition, $i = 4$. The right panel shows the corresponding decay time of the Rabi oscillations (τ_2). The microwave frequency was calibrated using a Ramsey sequence, and tuned exactly to resonance, and the microwave power at the input to the cavity was 26.8 dBm. Each pixel was fit using Eq. (2), and the microwave magnetic field strength was then calculated as described in Ref. [12]. The σ_- and σ_+ components were also imaged [12], with measured field strengths below $1.5\,\mu$T. The π component, whose dominance follows from the cavity design [11], is more than 3 times stronger, with field strengths up to $5\,\mu$T.

The lifetime, τ_2, of the Rabi oscillations is significantly shorter than the T_2 time, principally due to inhomogeneities in the microwave magnetic field [1]. This can be seen in Figure 6, where the τ_2 time is inversely correlated with the magnitude of the microwave magnetic field inhomogeneity, which in turn is linked to the field strength. The strong spatial variation in τ_2 highlights the importance of our technique for cell and cavity characterisation, in particular for high precision devices such as vapor cell atomic clocks.

V. Conclusions

We have used time-domain spatially resolved optical and microwave measurements to image atomic relaxation and the polarisation-resolved microwave magnetic field strength in a microfabricated Rb vapor cell placed inside a microwave cavity. The population and coherence relaxation times were measured to be uniform across the cell centre, with values at 90°C of $T_1 = 265\,\mu$s and $T_2 = 350\,\mu$s, respectively. Depolarising collisions between Rb atoms and the cell walls resulted in T_1 and T_2 times around $150\,\mu$s near the cell edge, and diffusion of these atoms lowered relaxation times within 0.7 mm of the cell wall. Images of the cavity microwave magnetic field show significant spatial inhomogeneity, due to perturbations to the cavity introduced by the dielectric cell material. For a given hyperfine transition, we can identify the cell region maximising the number of Rabi oscillations, and hence the region of optimal coherent manipulation.

Our measurement technique is fast, simple, and produces high resolution images for vapor cell and microwave-device characterisation. It is of particular interest for characterising cells in miniaturised atomic clocks and sensing applications. It is also of interest for characterising the cell and cavity properties in larger and high-performance vapor cell atomic clocks.

Acknowledgment

This work was supported by the Swiss National Science Foundation (SNFS) and the European Space Agency (ESA). We thank Y. Pétremand for filling the cell, and R. Schmied for discussions on the modelling of relaxation in the cell.

References

[1] M. Arditi and T. R. Carver, "Hyperfine Relaxation of Optically Pumped Rb^{87} Atoms in Buffer Gases," *Physical Review*, vol. 136, no. 3A, p. A643, 1964.
[2] D. Budker and M. Romalis, "Optical magnetometry," *Nature Physics*, vol. 3, pp. 227–234, 2007.
[3] B. Julsgaard, A. Kozhekin, and E. S. Polzik, "Experimental long-lived entanglement of two macroscopic objects." *Nature*, vol. 413, no. 6854, pp. 400–3, Sep. 2001.
[4] M. Pellaton, C. Affolderbach, Y. Pétremand, N. de Rooij, and G. Mileti, "Study of laser-pumped double-resonance clock signals using a microfabricated cell," *Physica Scripta*, vol. T149, p. 014013, May 2012.
[5] V. Shah, S. Knappe, P. D. D. Schwindt, and J. Kitching, "Subpicotesla atomic magnetometry with a microfabricated vapour cell," *Nature Photonics*, vol. 1, no. 11, pp. 649–652, Nov. 2007.
[6] I. Savukov, S. Seltzer, M. Romalis, and K. Sauer, "Tunable Atomic Magnetometer for Detection of Radio-Frequency Magnetic Fields," *Phys. Rev. Lett.*, vol. 95, no. 6, p. 063004, Aug. 2005.
[7] P. Böhi and P. Treutlein, "Simple microwave field imaging technique using hot atomic vapor cells," *Appl. Phys. Lett.*, vol. 101, no. 18, p. 181107, 2012.
[8] J. A. Sedlacek, A. Schwettmann, H. Kübler, R. Löw, T. Pfau, and J. P. Shaffer, "Microwave electrometry with Rydberg atoms in a vapour cell using bright atomic resonances," *Nature Physics*, vol. 8, no. 11, pp. 819–824, Sep. 2012.
[9] W. Ketterle, D. Durfee, and D. Stamper-Kurn, *Making, probing and understanding Bose-Einstein condensates...*, M. Inguscio, S. Stringari, and C. E. Wieman, Eds. IOS Press, Amsterdam, 1996.
[10] S. Micalizio, C. E. Calosso, A. Godone, and F. Levi, "Metrological characterization of the pulsed Rb clock with optical detection," *Metrologia*, vol. 49, no. 4, pp. 425–436, Aug. 2012.
[11] G. Mileti, I. Ruedi, and H. Schweda, *Proc. 6th European Frequency and Time Forum*, pp. 515–519, 1992.
[12] A. Horsley, G.-X. Du, M. Pellaton, C. Affolderbach, G. Mileti, and P. Treutlein, "Imaging of Relaxation Times and Microwave Field Strength in a Microfabricated Vapor Cell," *preprint arXiv:1306.1387*, 2013.
[13] W. Happer, "Optical pumping," *Reviews of Modern Physics*, vol. 44, no. 2, pp. 169–249, 1972.